

HIGH-RESOLUTION TOPOMAPPING OF MARS: LIFE AFTER MER SITE SELECTION. R. L. Kirk¹, E. Howington-Kraus¹, T. M. Hare¹, R. Soricone¹, K. Ross¹, L. Weller¹, M. Rosiek¹, B. Redding¹, D. Galuszka¹, B. A. Archinal¹, and A. F. C. Haldemann². ¹U.S. Geological Survey, (2255 N. Gemini Dr., Flagstaff, AZ 86001, rkirk@usgs.gov), ²Jet Propulsion Laboratory, California Institute of Technology (4800 Oak Grove Dr., Pasadena, CA, 91109, albert@shannon.jpl.nasa.gov).

Introduction: In this abstract we describe our ongoing use of high-resolution images from the Mars Global Surveyor Mars Orbiter Camera Narrow-Angle subsystem (MGS MOC-NA) [1] to derive quantitative topographic and slope data for the martian surface at 3–10-m resolution. Our efforts over the past several years [2, 3, 4] focused on assessment of candidate landing sites for the Mars Exploration Rovers (MER) and culminated in the selection of sites in Gusev crater and Meridiani Planum as safe as well as scientifically compelling. As of this writing, MER-A (Spirit) has landed safely in Gusev and we are performing a limited amount of additional mapping near the landing point to support localization of the lander and rover operations planning. The primary focus of our work, however, has been extending our techniques to sample a variety of geologic terrains planetwide to support both a variety of geoscientific studies and planning and data analysis for missions such as Mars Express, Mars Reconnaissance Orbiter, and Phoenix.

Methodology: Our techniques for stereomapping and photoclinometry (PC) are described in detail in a recent paper [4] and are similar to those used for a wide range of planetary datasets [5]. We use the USGS in-house digital cartographic software ISIS [6] for mission-specific data ingestion and calibration steps, as well as "2D" processing such as map-projection and image mosaicking. Photoclinometry [7,8] and slope analysis are also performed with (unreleased) programs that read ISIS image files. Our commercial digital photogrammetric workstation running SOCET SET ® BAE Systems software [9] is used for "3D" processing steps such as control of the images and automatic extraction and manual editing of DEMs. SOCET SET includes a pushbroom scanner sensor model that is physically realistic but "generic" enough to describe most MOC-NA (and WA) images and allows low-order adjustments to register the images to the globally adjusted MOLA coordinates [10]. Many MOC images are also affected by high-frequency pointing variations ("jitter") that cannot be corrected with the available software for image control. Jitter in the stereobase direction gives rise to topographic artifacts in the form of stripes across the DEM; these can be suppressed by highpass filtering. Severe jitter at right angles to the stereobase interferes with matching; a workaround is to segment the image into regions that can be controlled and DEMs collected separately. Development of bundle adjustment software incorporating high-frequency oscillations (see companion abstract [11]) will eventually eliminate the need for these time consuming *ad hoc* fixes. Estimates of the expected vertical precision (EP) and slope-measurement accuracy for a given stereopair can be derived from the image resolutions and geometry as described in [4].

The two-dimensional PC algorithm of Kirk [7] was used to construct DEMs of selected image regions with single-pixel resolution. Accuracy of these DEMs depends crucially on the validity of photometric assumptions [12]. Whereas the surface photometry of Mars is adequately constrained [13], the atmospheric haze contribution to any given image is essentially an unknown; mis-estimating this haze level leads to errors in the overall scale of topography (and slopes). We therefore calibrate the PC analysis by choosing a haze estimate that gives results consistent with stereogrammetry. This can be done in either the image or the topographic domain. By shading the stereo DEM with a realistic surface photometric function and comparing the result to the image, one obtains the haze estimate as the constant offset in a regression between the two. Conversely, trial PC can be done with different haze values and the case that gives best agreement between PC and stereo DEMs selected [8]. In either method errors in the stereo DEM limit the resemblance to the image and can make the comparison difficult. Tests with simulated and real data suggest that photoclinometry can be calibrated to 10–20% relative accuracy for height differences and slopes [4].

Landing Sites and Other Sites: On 3 January 2004, Spirit landed at a location established by radio tracking as approximately 175.478°E, 14.571°S (E. Graat, written communication, 5 January 2004). This is well within the landing uncertainty ellipse but outside any of the MOC stereopairs we had previously mapped [2, 3, 4]. We have made spot height measurements and are attempting to construct a DEM from the stereopair listed in Table 1, which covers the 50–100-m high hills visible from the lander about 2 km to the southeast, and has excellent stereo geometry but substantial surface changes and saturated data in the second image. We intend to map other MOC pairs in the immediate vicinity of Spirit as they are acquired, as well

as pairs near MER-B (Opportunity) when it lands in Meridiani Planum, and will report on the results in our poster.

Table 1—MOC Stereopairs Mapped after MER Site Selection

Image 1	Image 2	E Lon (°)	Lat (°)	Description
E0300012 3.49/0.34	E1601962 3.58/17.93	175.3	-14.6	Gusev crater: hills SE of Spirit landing point
SP123503 2.61/31.48	SP125403 2.50/22.32	311.7	22.3	Chryse Planitia: just SW of VL 1 point
E1101658 1.87/18.00	E1801397 1.87/17.96	134.1	47.7	Utopia Planitia: just SW of VL 2 point
FHA00541 1.48/0.13	E0402223 1.97/19.72	358.5	2.1	Meridiani Planum: rough lava flow
R0300370 3.04/17.67	R0600195 2.04/33.68	13.8	-0.9	Schiaparelli crater: layered sediments
M1500319 5.76/0.29	E1401039 5.01/18.16	326.2	-24.2	Holden crater: braided channels in delta
M0300772 5.94/0.14	E1500790 3.69/18.03	324.5	26.7	Chryse Planitia; secondary crater field
M1900916 3.41/0.33	E1800785 3.44/29.29	351.5	-53.5	MARSIS: low roughness
M0402989 2.85/0.30	E1501190 4.38/17.97	331.3	-51.4	MARSIS: high roughness
M1000099 5.70/0.28	E1103126 5.84/18.03	312.9	-57.7	MARSIS: high hydrogen

Resolution (m/pixel), emission angle (°) are listed under image ID

Table 1 also lists six stereopairs in locations of scientific interest outside the MER landing sites that were mapped in 2003. The primary interest of the Viking Lander (VL) 1 and 2 sites is the potential to compare our slope-statistical results with "ground truth" from the landers [14] as we have done previously at the Mars Pathfinder site [2, 3, 4] and expect to do with Spirit and Opportunity. The VL 2 site is also being studied as an analogue for potential Phoenix landing sites in similarly textured terrain farther north (R. Arvidson, written comm., 2003). The other sites mapped include extremely rugged terrain interpreted as lava flows in Meridiani Planum, braided channels in a fossil delta in Holden crater, sedimentary layers in a 2.3-km crater in Schiaparelli, and a field of secondary craters near the VL 1 site. The landforms and stratigraphy in the Meridiani and Holden examples are sufficiently complex that perspective visualizations computed from the DEMs are a significant aid in interpreting the images. The main interest in Schiaparelli is the thickness of the sediments: relief at the edge of the deposit is ≤ 5 m, and individual layers appear to be substantially thinner than this and possibly to conform to the crater floor. The final model is of interest because past studies have indicated that small fresh craters on Mars are typically shallower than small primary craters on the Moon and similar in depth to lunar secondary craters [15]. Measurement of the depth of these craters, which are traceable to a well-preserved primary at 22.6°N, 321.4°E may help distinguish between the alternative hypotheses that martian primary craters are unusually shallow or that the majority of small craters on Mars are in fact secondary.

A Global Database of Validated MOC-NA Stereopairs: A critical step in topomapping with MOC-NA images is identifying suitable stereopairs, which can be difficult because the images are numerous but small and their catalogued positions are based on predicted spacecraft data and are uncertain at the 1–2-km level (i.e., a substantial fraction of the swath width). Our mapping of the candidate MER sites relied on maps of MOC coverage produced by the site selection working group [16], and the majority of the pairs described above were identified in MOC team press releases (available online at www.msss.com/mars_images/moc/index.html). In order to extend our mapping capability to other areas of the planet, we populated a GIS database with metadata taken from the cumulative index file released with the images. This database incorporated 45,342 NA images through mission phase E22 with resolutions ≤ 10 m/pixel. Pairs of potentially overlapping images were next identified; in order to allow for possible worst-case errors in the image positions, the footprints contained in the cumulative index were expanded by 2 km before the intersection calculation was performed. Those candidate pairs in which the illumination geometry of the images was too dif-

ferent for stereomatching to be likely to succeed (by the same criteria we have used in the past to identify useful stereopairs of Viking Orbiter images [17]) were eliminated automatically. Pairs consisting of two nadir (vertical) images were likewise eliminated. The result was a list of 5242 nadir-oblique image pairs, and a smaller set of ~1400 oblique-oblique pairs. A subset of the second list actually consist of same-side oblique images rather than useful stereo and can also be eliminated automatically by calculating the total parallax/height ratio of the pairs from the three-dimensional imaging geometry.

To date, we have focused our efforts on the nadir-oblique pairs. We are visually inspecting them and eliminating pairs which do not actually overlap, as well as those with extensive noisy or dropped data, high atmospheric haze, or major surface albedo changes between the images, all of which would prevent successful stereomatching. At the same time, we recorded the amount of cross-track overlap between the images of each pair (to the nearest 10%) and a brief description of the surface morphology. The number of validated pairs are tabulated by region (corresponding to the quadrangles of the USGS 1:5,000,000-scale "Mars Chart" map series) and amount of cross-track overlap in Table 2. and their locations are plotted in Figure 1. Note that the south polar region (MC-30), which contains an unusually large number of candidate pairs, is still being checked at this writing. Nevertheless, ~300 completely overlapping pairs and more than 300 additional with ≥50% overlap have already been identified. We will include the pairs found in MC-30 and oblique-oblique pairs found in our poster, and the full list of pairs will be made available (both as a flat file and as GIS layers) online when completed. We also intend to update this database periodically as additional MOC-NA images are released.

Table 2—Validated MOC-NA Stereopairs

Region MC-	Percent Image Overlap										Totals
	10	20	30	40	50	60	70	80	90	100	
1	6	1	2	2	5	1	7	4	4	21	53
2		2					2	1	2	3	10
3							2	1	3	3	9
4	2			1		1	1	1	2	3	11
5	2	3	1	5	3	2	1	4	4	8	33
6	1	2	2		1		2	4	4	6	22
7					1		2	2	2	10	17
8	3	1	1	1	1	1	2	6	8	12	36
9	1	6		2	1	6	7	3	7	6	39
10	4	5	1	1	1	2	2	1	4	8	29
11	2		1	5	1	6	7	3	10	22	57
12	1			2	4	7	2	1	4	15	36
13		1	1	3	5	3	3	6	7	13	42
14		1	1	2	2		1	1	1	7	16
15											0
16	1	1	3		1		1	1	2	8	18
17				4	1	2	3	1	3	8	22
18		1			1					31	33
19	1	2	1	1	1	4		1	6	8	25
20	1	5	1	3	3	1	3	4	1	8	30
21	2	2			3	2	2	1	9	8	29
22	3	1			1	1		1	5	4	16
23			3	5	3		4	2	4	7	28
24	2	1	1	1	4	1	4	8	3	9	34
25				1	2		2	1	2	3	11
26	1	2		1	3	2	3	4	4	10	30
27			4	1	5	3	2	1	7	26	49
28				2	2		1	1	5	16	27
29	1								1	3	5
Totals	34	37	23	43	55	45	66	64	114	286	767

Validation of images in MC-30 was incomplete at time of writing.

Critical Products for Future Missions: By using the database just described, we can identify MOC stereopairs planetwide, and can use the stereo coverage to sample terrains with specific properties as desired. Under the Mars Critical Data Products Initiative, we are using this capability to produce DEMs and slope statistical models to support future missions. One of these missions is the Phoenix lander; as noted above, we have mapped the VL 2 site as an analogue but mapping of the actual landing zone awaits the acquisition

Any use of trade, product, or firm names is for commercial purposes only and does not imply endorsement by the U.S. Government.

of suitable imagery in the near future. The other primary customers are the radar instruments MARSIS soon to be deployed on orbit by Mars Express, and SHARAD on the Mars Reconnaissance Orbiter to be launched in 2005. Radar observations are influenced by a large number of parameters, including electrical properties, surface slopes over distances exceeding the wavelength (leading to "quasi-specular scattering"), surface roughness at the wavelength and shorter scales, and subsurface discontinuities and other inhomogeneities. MARSIS and SHARAD are both ground-penetrating radars, with the primary objective of sounding below the surface of Mars to determine the distribution of ice and liquid water, as well as the extent of the geologic layering [18, 19]. Thus, these instruments view surface scattering mainly as interference that must be understood and modeled in order to map what lies beneath. Our DEMs with resolutions of meters and slope accuracies of a fraction of a degree [4] will allow the radar instrument teams to model quasi-specular surface scattering for a wide variety of terrains, both before receipt of radar data in order to understand the impact of such scattering on their signal and hence optimize operational parameters, and during the mission as part of the analysis of their data. To date, we have identified MOC stereopairs within 5 km of predicted MARSIS night-side ground tracks and in areas with radial magnetic field strengths ≤1 nT [20]. Of these candidates, we selected three for mapping (Table 1) having respectively the highest and lowest roughness as measured by MOLA pulsewidth [21] and the highest subsurface hydrogen content as measured by the Mars Odyssey Gamma Ray Spectrometer [22]. These sites are now being mapped and results will be reported in our poster. Additional pairs will be chosen by similar criteria for SHARAD and mapped later in 2004.

Acknowledgements: The work described here was supported by the Mars Exploration Rovers Mission, the Mars Fundamental Research Program, and the Mars Critical Data Products Initiative.

References: [1] Malin, M. C., and Edgett, K. S. 2001, *JGR 106(E10)* 23429. [2] Kirk, R. L., et al. 2002, *LPS XXXIII*, 1988. [3] Kirk, R. L., et al. 2003, *LPS XXXIV*, 1966. [4] Kirk, R. L. et al. 2004, *JGR*, in press. [5] Kirk, R. L., et al. 2000, *IAPRS XXXIII(B4)*, 476 (CD-ROM). [6] Eliason, E. 1997, *LPS XXVIII*, 331; Gaddis, L. et al. 1997, *LPS XXVIII*, 387; Torson, J. and Becker, K. 1997, *LPS XXVIII*, 1443; isis.astrogeology.usgs.gov [7] Kirk, R. L. 1987, *III. A fast finite-element algorithm for two-dimensional photogrammetry*. Ph.D. Thesis (unpubl.), Caltech. [8] Kirk, R. L. et al. 2003, ISPRS Working Group IV/9 Workshop "Advances in Planetary Mapping 2003", Houston, March 2003, abstract online at http://astrogeology.usgs.gov/Projects/ISPRS/Meetings/Houston2003/abstracts/Kirk_isprs_mar03.pdf. [9] Miller, S. B. and Walker, A. S. 1993, *ACSM/ASPRS Annual Convention and Exposition Technical Papers*, 3, 256; Miller, S. B. and Walker, A. S. 1995, *Z. Photograph. Fernerkundung*, 1/95, 4. [10] Smith, D. E., et al. 2001, *JGR 106(E10)*, 23689; Neumann, G. A., et al. 2001, *JGR 106(E10)*, 23753. [11] Archinal, B. A., et al. this conference. [12] Kirk, R. L., et al., 2001, *LPS XXXII*, 1874. [13] Kirk, R. L., et al. 2000, *LPS XXXI*, 2025. [14] Seelos, F., et al. 2002, *LPS XXXIII*, 1945. [15] Hurst, M., et al., this conference. [16] Golombek, M. P., et al. 2004, *JGR 108(E12)*, 8072. [17] Kirk, R. L., et al. 1999, *LPS XXX*, 1857. [18] Martin, P. D., et al. 2001, *LPS XXXII*, 1575. [19] Ori, G. G., et al. 2002, *LPS XXXIII*, 1503. [20] Connerney, J. E. P., et al. 2001, *GRL*, 28(21), 4015 [21] Neumann, G. A. et al. 2003, *GRL*, 30(11), 1561. [22] Feldman, W, et al. 2002, *Science*, 297, 75.

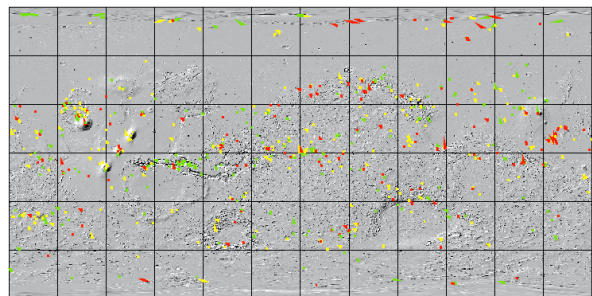


Figure 1. Distribution of validated MOC-NA oblique/nadir stereopairs tallied in Table 2. Red: 10–40% overlap. Yellow: 50–90%. Green: 100%. Footprints enlarged for clarity. Projection is global simple cylindrical, north up, center longitude 0°, with 30° grid.